Outside-Xylem Vulnerability, Not Xylem Embolism, Controls Leaf Hydraulic Decline during Dehydration[1][CC-BY]

Christine Scoffoni*, Caetano Albuquerque, Craig R. Brodersen, Shatara V. Townes, Grace P. John, Megan K. Bartlett, Thomas N. Buckley, Andrew J. McElrone, and Lawren Sack

Department of Ecology and Evolutionary Biology, University of California, Los Angeles, California, 90095 (C.S., S.V.T., G.P.J., M.K.B., L.S.); Department of Biology, Utah State University, Logan, Utah 84322 (C.S.); Department of Viticulture and Enology, University of California, Davis, California 95616 (C.A., A.J.M.); School of Forestry and Environmental Studies, Yale University, New Haven, Connecticut 06511 (C.R.B.); IA Watson Grains Research Centre, Plant Breeding Institute, Sydney Institute of Agriculture, University of Sydney, Narrabri, New South Wales 2390, Australia (T.N.B.); and United States Department of Agriculture-Agricultural Research Service, Davis, California 95616 (A.J.M.)

ORCID IDs: 0000-0002-2680-3608 (C.S.); 0000-0001-6222-3996 (C.A.); 0000-0002-0924-2570 (C.R.B.); 0000-0002-8045-5982 (G.P.J.).

Leaf hydraulic supply is crucial to maintaining open stomata for CO_2 capture and plant growth. During drought-induced dehydration, the leaf hydraulic conductance (K_{leaf}) declines, which contributes to stomatal closure and, eventually, to leaf death. Previous studies have tended to attribute the decline of K_{leaf} to embolism in the leaf vein xylem. We visualized at high resolution and quantified experimentally the hydraulic vulnerability of xylem and outside-xylem pathways and modeled their respective influences on plant water transport. Evidence from all approaches indicated that the decline of K_{leaf} during dehydration arose first and foremost due to the vulnerability of outside-xylem tissues. In vivo x-ray microcomputed tomography of dehydrating leaves of four diverse angiosperm species showed that, at the turgor loss point, only small fractions of leaf vein xylem conduits were embolized, and substantial xylem embolism arose only under severe dehydration. Experiments on an expanded set of eight angiosperm species showed that outside-xylem hydraulic vulnerability explained 75% to 100% of K_{leaf} decline across the range of dehydration from mild water stress to beyond turgor loss point. Spatially explicit modeling of leaf water transport pointed to a role for reduced membrane conductivity consistent with published data for cells and tissues. Plant-scale modeling suggested that outside-xylem hydraulic vulnerability can protect the xylem from tensions that would induce embolism and disruption of water transport under mild to moderate soil and atmospheric droughts. These findings pinpoint outside-xylem tissues as a central locus for the control of leaf and plant water transport during progressive drought.

Leaves account for the bulk of photosynthetic productivity and transpirational water use, and given the increasing incidence and severity of droughts in many regions (Vicente-Serrano et al., 2014; Diffenbaugh et al., 2015) if not globally (Sheffield et al., 2012), the mechanisms underlying the drought responses of leaves are ever more critical to understand. Reduction of photosynthesis and growth under mild dehydration and subsequent death under prolonged drought are primarily related to failure of the water-transport system (Tyree and Zimmermann, 2002; Sack et al., 2016a). Water moves under negative pressure through plant xylem, via the cohesion-tension mechanism (Dixon and Joly, 1895), and a certain level of tension can cause air to aspirate through a xylem conduit, causing spontaneous vaporization, a process known as cavitation. The resulting embolization of the xylem conduits has been widely believed to be the main cause of hydraulic decline during drought (Milburn, 1966; Tyree and Zimmermann, 2002), which results in declines in gas-exchange rates (Nardini and Salleo, 2000; Brodribb and Holbrook, 2003; Hernandez-Santana et al., 2016) and can ultimately precipitate plant mortality (Choat et al., 2012). While embolism is a major cause of the failure of stem hydraulic function, its role in leaves has not yet been clarified. Understanding the role of embolism on leaf hydraulic function is equally if not more important

[1] This work was supported by the U.S. National Science Foundation (grant nos. 1146514 and 1457279), the Australian Research Council (grant nos. DP150103863 and LP130101183), the U.S. Department of Agriculture-Agricultural Research Service Current Research Information System (grant no. 5306 21220-004-00), CAPES/Brazil, the NIFA Specialty Crops Research Initiative, and the American Vineyard Foundation; the Advanced Light Source is supported by the Office of Science, Office of Basic Energy Sciences, U.S. Department of Energy (grant no. DE-AC02-05CH11231).

* Address correspondence to cscoffoni@ucla.edu.

The author responsible for distribution of materials integral to the findings presented in this article in accordance with the policy described in the Instructions for Authors (www.plantphysiol.org) is: Christine Scoffoni (cscoffoni@ucla.edu).

C.S., C.R.B., A.M., and L.S. designed experiments; C.S., C.A., S.V.T., G.P.J., M.K.B., T.N.B., and A.J.M. performed experiments and simulations; C.S., C.A., and C.R.B. analyzed data; C.S. and L.S. wrote the article with contributions from all authors.

www.plantphysiol.org/cgi/doi/10.1104/pp.16.01643

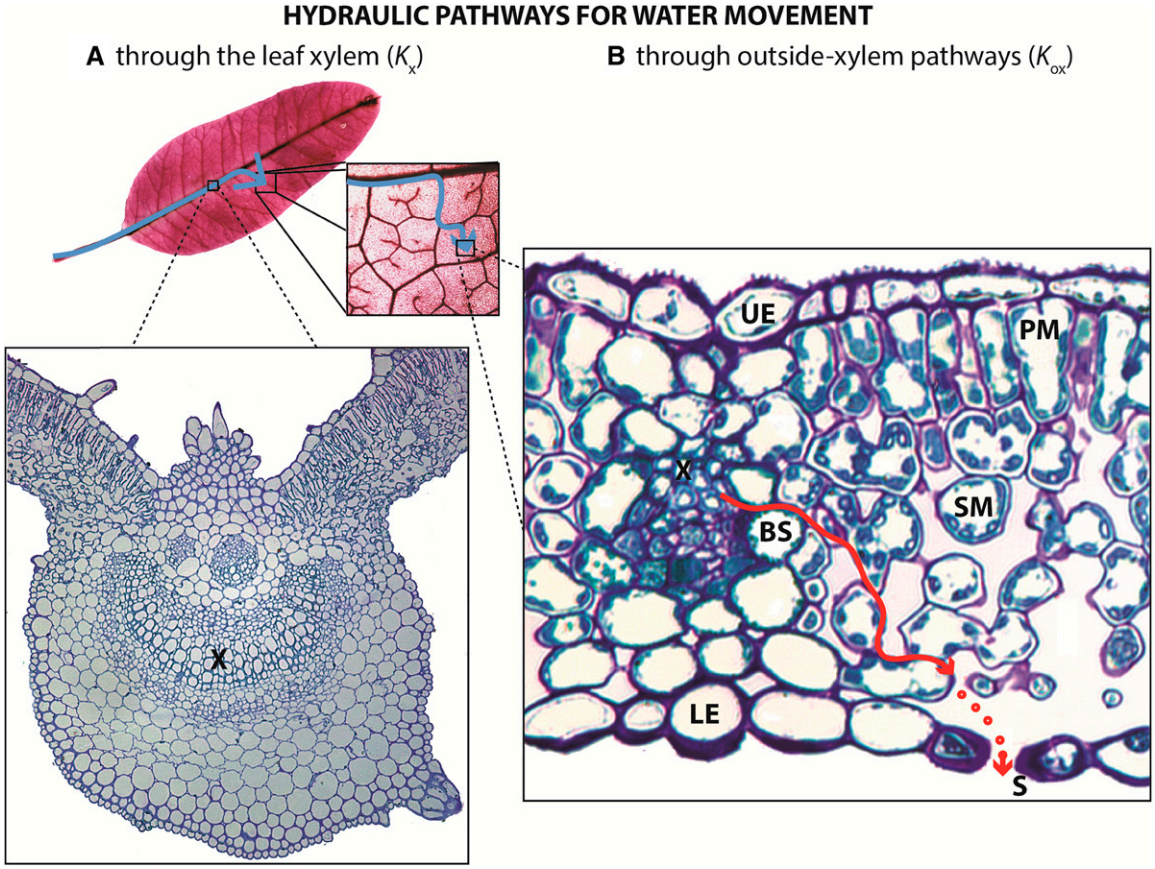

Figure 1. K_{leaf} characterizes the water-transport capacity of the whole leaf and is influenced by water movement through the leaf xylem (K_x; A) and through the mesophyll, or outside-xylem pathways (K_{ox}; B), which includes vascular parenchyma, bundle sheath, and mesophyll cell pathways for liquid and/or vapor phase transport and diffusion through air spaces (red dots) through stomata. As the leaf dehydrates, observed declines in K_{leaf} have typically been attributed primarily to reduction of K_x due to the formation of embolism in xylem conduits, although recent studies suggested a possible role for changes in outside-xylem pathway properties via reduced membrane permeability and cell shrinkage. Symbols are as follows: xylem (X), bundle sheath cell (BS), spongy mesophyll cell (SM), palisade mesophyll cell (PM), upper epidermal cell (UE), lower epidermal cell (LE), and stomata (S).

than in stems, as leaves represent a hydraulic bottleneck (Sack and Holbrook, 2006) that can determine plant hydraulic responses and the resulting declines in stomatal conductance and photosynthesis during drought (Brodribb and Holbrook, 2003; Sack and Holbrook, 2006). Leaves are highly vulnerable to dehydration, with leaf hydraulic conductance (K_{leaf}) often declining rapidly between full turgor and turgor loss point and even more strongly during extreme dehydration (Brodribb and Holbrook, 2006; Johnson et al., 2009b; Scoffoni et al., 2012; Sack et al., 2016b). This response could arise in one or more of several tissues, as water moves first through the vein xylem, then exits the xylem through bundle sheath cells and flows through the mesophyll before evaporating into the intercellular air space, and then diffusing through stomata out of the leaf (Fig. 1; Tyree and Yianoulis, 1980; Boyer, 1985; Rockwell et al., 2014). Thus, the decline of K_{leaf} with dehydration may be driven not just by reduced vein xylem hydraulic conductance (K_x) but also by reduced outside-xylem hydraulic conductance (K_{ox}), which includes pathways through the vascular parenchyma, the bundle sheath, and the rest of the mesophyll tissues. Both K_x and K_{ox} determine K_{leaf}:

$$K_{leaf} = \left(K_x^{-1} + K_{ox}^{-1}\right)^{-1} \quad (1)$$

Indeed, recent studies have suggested that cell shrinkage with dehydration, and/or deactivation of membrane aquaporins outside the xylem, could strongly reduce K_{leaf} (Kim and Steudle, 2007; Shatil-Cohen et al., 2011; Pantin et al., 2013; Scoffoni et al., 2014; Moshelion et al., 2015; Sade et al., 2015). Yet, the vulnerability of K_x and K_{ox}, and their influences on K_{leaf} decline with dehydration, have not been clearly disentangled. Although recent evidence has suggested that the leaf xylem is resistant to embolism under moderate levels of dehydration (Scoffoni and Sack, 2015; Bouche

et al., 2016; Brodribb et al., 2016a), whole-leaf hydraulic decline with dehydration has been most often primarily attributed to embolism, based on indirect evidence (Milburn and Johnson, 1966; Crombie et al., 1985; Kikuta et al., 1997; Nardini and Salleo, 2000, 2003; Salleo et al., 2000, 2001; Nardini et al., 2001, 2003, 2008; Bucci et al., 2003; Lo Gullo et al., 2003; Stiller et al., 2003; Trifilò et al., 2003a; Brodribb and Holbrook, 2005; Woodruff et al., 2007; Johnson et al., 2009a, 2012; Blackman et al., 2010, 2014). For instance, the earliest report of xylem embolism was for leaf petioles, based on acoustic emissions thought to be caused by cavitation events (Milburn, 1966), and subsequent studies reported that the number of acoustic emissions a leaf generates correlated with leaf hydraulic decline (Tyree and Sperry, 1989; Johnson et al., 2009a). However, it is now recognized that acoustic emissions from drying leaves may arise from processes other than xylem conduit embolism, such as fractures in the tissues or embolism within fibers or mesophyll cell walls (Sandford and Grace, 1985; Ritman and Milburn, 1988; Cochard et al., 2013). In severely dehydrated excised leaves, embolisms can be observed in the leaf vein xylem using scanning electron microscopy of cryogenized sections, dye methods, or direct light transmission, and several studies reported that K_{leaf} decline corresponded to the accumulation of leaf vein embolism (Cochard et al., 2000; Nardini et al., 2003; Trifilo et al., 2003b; Woodruff et al., 2007; Johnson et al., 2009a; Brodribb et al., 2016b) and suggested this to be the main driver of K_{leaf} decline. However, there has been a lack of information of the number of embolized xylem conduits within given vein orders across the range of leaf water stress and their influence on K_{leaf} (Wylie, 1947; McKown et al., 2010; Sack and Scoffoni, 2013) relative to the potentially strong role of vulnerability of the outside-xylem pathways. Recent work has proposed that outside-xylem hydraulic decline may play a role in K_{leaf} decline (Sade et al., 2014; Scoffoni et al., 2014; Hernandez-Santana et al., 2016; Trifiló et al., 2016). A study that partitioned the vulnerability of K_{leaf} into that of K_x and K_{ox} (Trifiló et al., 2016) found that both contributed, depending on species, but measurements were made under low irradiance, which would minimize the response of K_{ox} before the turgor loss point (Guyot et al., 2012; Sack et al., 2016b). A strong test of the relative roles of K_x and K_{ox} depends on their determination for illuminated leaves coupled with direct observations of the formation of emboli in the xylem.

To test the relative roles of xylem embolism and changes in outside-xylem properties in determining the decline in K_{leaf} during dehydration, we combined three approaches. We first investigated whether embolism occurred in leaf veins as leaves dehydrated to turgor loss and beyond using x-ray microcomputed tomography (microCT). We then quantified the vulnerability of K_x and K_{ox} to dehydration, which allowed us to partition their influence on the vulnerability of K_{leaf} at any point during dehydration under high irradiance. We investigated the anatomical determinants of the

Table I. *Study species, family, origin, plant and leaf habit, and mean values ± SE for hydraulic vulnerability traits: water potential at which K_{leaf}, K_x, and K_{ox} declined by 50% (P_{50}) and 88% (P_{88}), and the turgor loss point (Ψ_{TLP})*

Species	Family	Origin	Plant Habit	Leaf Habit	$P_{50,Kleaf}$ and $P_{88,Kleaf}$	$P_{50,Kox}$ and $P_{88,Kox}$	$P_{50,Kx}$ and $P_{88,Kx}$	Ψ_{TLP}
					MPa	*MPa*	*MPa*	*MPa*
Cercocarpus betuloides	Rosaceae	California, Mexico	Tree	Evergreen	−2.8, −6.5	−2.8, −6.2	−3.0, −6.6	−2.6 ± 0.04
Comarostaphylis diversifolia	Ericaceae	California, Mexico	Tree	Evergreen	−2.8, −5.0	−2.7, −5.0	−5.6, −8.4	−3.4 ± 0.34
Hedera canariensis	Araliaceae	Canary Islands	Shrub	Evergreen	−0.64, −1.5	−0.58, −1.3	−1.9, −2.8	−2.0 ± 0.07
Lantana camara	Verbenaceae	Pantropical	Shrub	Deciduous	−0.80, −1.8	−0.79, −1.8	−0.87, −1.6	−1.4 ± 0.04
Magnolia grandiflora	Magnoliaceae	Southern United States	Tree	Evergreen	−0.42, −4.1	−0.33, −2.6	−3.3, −4.6	−2.1 ± 0.02
Malosma laurina	Anacardiaceae	California, Mexico	Shrub	Evergreen	−0.64, −1.4	−0.35, −0.95	−2.6, −5.2	−2.2 ± 0.06
Quercus agrifolia	Fagaceae	California, Mexico	Tree	Evergreen	−2.4, −4.2	−2.2, −4.1	−5.4, −6.7	−3.0 ± 0.12
Salvia canariensis	Lamiaceae	Canary Islands	Shrub	Evergreen	−0.26, −0.76	−0.09, −0.36	−0.89, −1.6	−1.2 ± 0.05

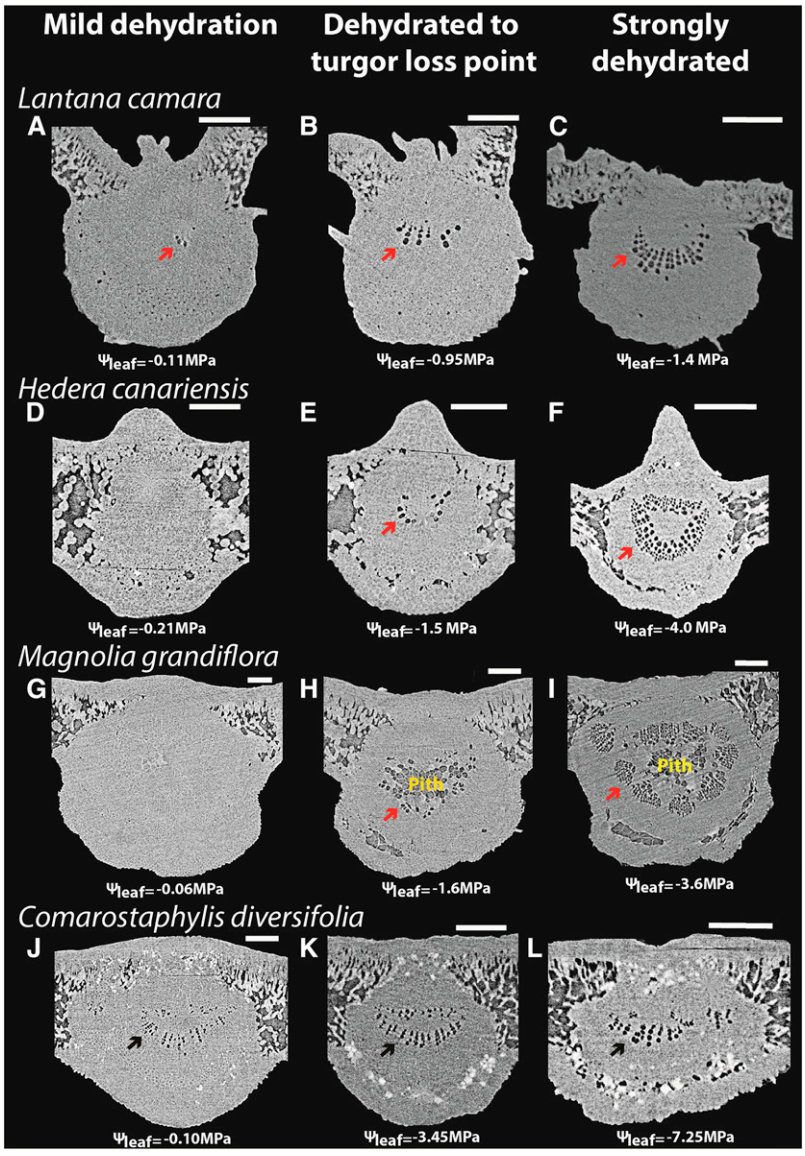

Figure 2. Low vulnerability of the leaf xylem to embolism before the turgor loss point as revealed by in vivo imaging of leaves of four diverse angiosperm species subjected to progressive dehydration (i.e. increasingly negative leaf water potential [Ψ_{leaf}]) using microCT. Scans show leaf midribs at mild dehydration, the turgor loss point, and extreme dehydration (an illustrative image for each range is shown from left to right), showing very few embolized midrib conduits above the turgor loss point. No emboli were observed in higher order veins above the turgor loss point, and few were observed even in extremely dehydrated leaves (data not shown). Note that *C. diversifolia* contains embolized protoxylem conduits, which are hydraulically nonfunctional, even for well-hydrated leaves, and these protoxylem conduits are included in the calculations of embolized conduits. Bars = 250 μm.

decline in outside-xylem pathways using a spatially explicit model of leaf water transport. Finally, we tested the implications of our findings, using a model of the whole-plant hydraulic system to estimate the influence of the measured declines of K_x, K_{ox}, and K_{leaf}, on whole-plant hydraulic conductance under different drought scenarios.

RESULTS

The main determinant of K_{leaf} decline in dehydrating leaves was hydraulic vulnerability of the outside-xylem pathways, rather than xylem embolism, for eight angiosperm species from eight families (Table I). The strong declines of K_{leaf} during progressive dehydration above and below the turgor loss point did not reflect patterns of xylem embolism observed in vivo (Figs. 2 and 3). MicroCT imaging of dehydrating leaves of four species revealed few gas-filled conduits even at the turgor loss point when K_{leaf} had already declined by over 60% (Figs. 2 and 3), where, on average, only 5% to 8.5% of midrib conduits were embolized across species in the midrib and none in the minor veins (Table II). Substantial levels of embolism (a maximum of 44% across species) were observed in the midrib only under extreme dehydration beyond the turgor loss point (Table II), but emboli were nonexistent or rare in the minor veins of these species at those extreme water potentials (Scoffoni et al., 2017). Hydraulic measurements of K_x vulnerability across the four species used for microCT imaging and an additional four ecologically diverse species (Table I) corroborated the microCT evidence of low K_x vulnerability on average across species compared with K_{leaf}. Thus, the water potential inducing 50% loss of hydraulic conductance for the leaf

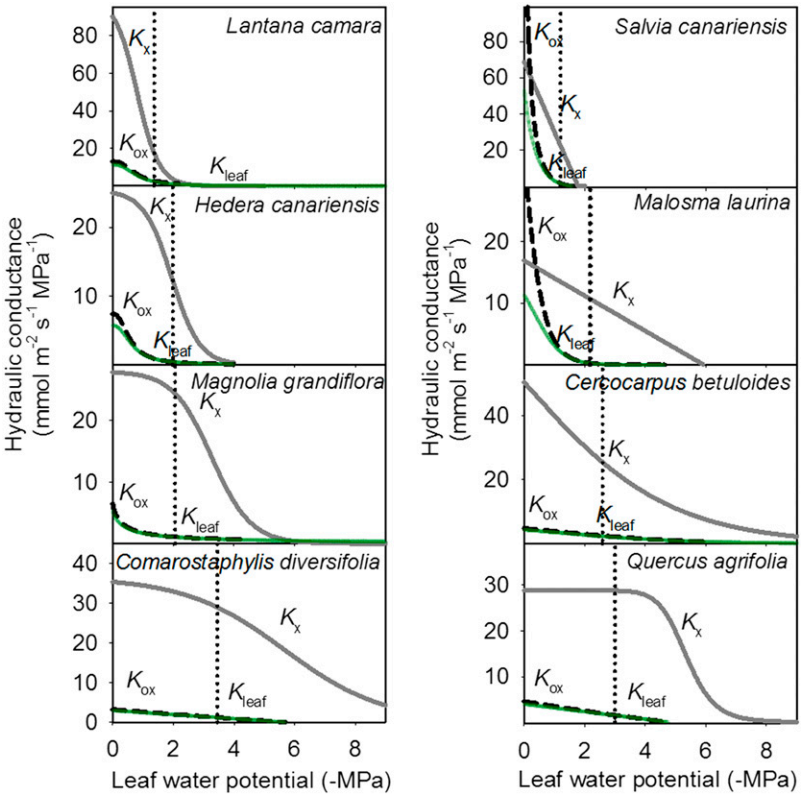

Figure 3. The vulnerability of K_{leaf} (green lines) to dehydration is determined mainly by the vulnerability of the outside-xylem pathways (K_{ox}; dashed black lines) and not that of the xylem (K_x; light-gray lines) across the four species for which microCT was performed (left) and an additional expanded set of four diverse species (right). The maximum likelihood function is plotted for each vulnerability curve (see "Materials and Methods"). The turgor loss point for each species is represented by the vertical dotted black line.

xylem ($P_{50,Kx}$; obtained from the K_x vulnerability curves shown in Supplemental Fig. S1) was, on average, 1.6 MPa more negative than that for the whole leaf ($P_{50,Kleaf}$; Fig. 3), representing a much lower sensitivity to water stress of K_x than of either K_{leaf} or K_{ox} (P values of 0.015 and 0.007, respectively, by paired Student's t test for each species; values for $P_{50,Kx}$, $P_{50,Kox}$, and $P_{50,Kleaf}$ are shown in Table I). By contrast, the water potential inducing 50% loss of hydraulic conductance for the outside-xylem pathways ($P_{50,Kox}$) was, on average, 0.1 MPa less negative than $P_{50,Kleaf}$, representing only a slightly greater sensitivity. Although the vulnerability of K_x to dehydration was much smaller than that of K_{ox} for all species, their relative sensitivities varied: the $P_{50,Kx}$ ranged from only 0.08 to 0.8 MPa more negative than $P_{50,Kox}$ in two soft-leaved shrub species (*Lantana camara* and *Salvia canariensis*) to 2.9 to 3.2 MPa more negative in sclerophyllous species of the California chaparral (*Comarostaphylis diversifolia* and *Quercus agrifolia*). Partitioning the contributions of xylem and outside-xylem pathways to the decline of K_{leaf} (see "Materials and Methods") showed that, across species, the decline in K_{ox} explained 86% to 100% of the decline in K_{leaf} at the turgor loss point (96% on average across species), 95% to 100% of that at $P_{50,Kleaf}$ (98% on average), and 75% to 100% of that at water potentials inducing 88% loss of leaf hydraulic conductance ($P_{88,Kleaf}$; 93% on average; Table III). Furthermore, while across species both $P_{50,Kx}$ and $P_{50,Kox}$ correlated positively with $P_{50,Kleaf}$ (r^2 = 0.57 and 0.99, respectively), when testing models predicting $P_{50,Kleaf}$ from $P_{50,Kox}$ and/or $P_{50,Kx}$, the model with $P_{50,Kox}$ alone was selected by maximum likelihood as the better predictor (Supplemental Table S1), explaining 81% of $P_{50,Kleaf}$ variation across species according to independent effects analysis.

Our model simulations of the plant hydraulic-stomatal system showed that, on average, across species (Fig. 4), and for three of four species individually (Supplemental Fig. S2; Supplemental Table S2), decline of K_{ox} would be the main determinant of the decline of not only K_{leaf} but of whole-plant hydraulic conductance under a wide range of scenarios of atmospheric drought (i.e. VPD) or soil drought (i.e. increasingly negative soil water potential [Ψ_{soil}]). Indeed, the trajectory of the percentage loss of conductivity of the whole-plant hydraulic system to either type of drought showed strong overlap with that of K_{ox}, while the bottleneck imposed by low K_{ox} shielded the leaf and stem xylem hydraulic conductances from tensions that would result in significant declines in these components under increasing VPD or increasingly negative Ψ_{soil}. Roots also have water flowing through living tissues of the outside-xylem component, and root hydraulic conductance (K_{root}) shows steep hydraulic vulnerability (Brodribb and Hill, 2000; Hacke et al., 2000; North et al., 2004), but K_{root} too is shielded from decline under increasing VPD by the bottleneck imposed by declining leaf K_{ox}. Notably, like the other compartments, K_{root} strongly declines under more negative Ψ_{soil}. However, because

Table II. *Percentage of embolized midrib conduits (%EMC) obtained from microCT imaging at three water potential intervals*
Mean ± SE are given, with the number of measured leaves indicated in parentheses.

Species	Mild Dehydration		Dehydration to Turgor Loss Point		Strong Dehydration	
	Water Potential	%EMC	Water Potential	%EMC	Water Potential	%EMC
	MPa		*MPa*		*MPa*	
C. diversifolia	−1.14 ± 0.56	4.84 ± 0.69 (5)	−3.37 ± 0.06	5.68 ± 0.60 (3)	−7.31 ± 0.53	5.27 ± 0.87 (4)
H. canariensis	−0.24 ± 0.04	5.56 ± 2.25 (5)	−1.61 ± 0.08	8.51 ± 2.25 (3)	−3.13 ± 0.36	19.6 ± 10.9 (4)
L. camara	−0.51 ± 0.22	6.30 ± 2.59 (4)	−1.07 ± 0.01	6.40 ± 0.13 (2)	−1.34 ± 0.04	36.8 ± 15.8 (3)
M. grandiflora	−0.06 ± 0.006	0.88 ± 1.83 (3)	−1.35 ± 0.30	4.96 ± 2.18 (3)	−5.64 ± 0.85	43.9 ± 21.9 (5)

Ψ_{soil} is less negative than leaf water potential during transpiration, K_{root} does not decline as strongly as leaf K_{ox} on average across species. Even for *L. camara*, which has a relatively vulnerable xylem, under increasing VPD, the decline of K_{ox} is steep and protects the other compartments of the plant from high tensions as for the other species, although under soil drought, steep declines in hydraulic conductances would occur in all organs (Supplemental Fig. S2).

Across species, the vulnerability of the hydraulic pathways correlated with the drought tolerance of the mesophyll cells. Thus, bulk leaf turgor loss point (Ψ_{TLP}) correlated with $P_{50,Kox}$ and $P_{50,Kx}$ (r^2 = 0.69 and 0.91, respectively; $P \leq 0.01$).

We applied model simulations to refine hypotheses for the source of the decline of K_{ox} in dehydrating leaves. We parameterized the MOFLO model for water transport outside the xylem (Buckley et al., 2015) with shifts in leaf anatomy and physiology that can be observed directly or that were determined experimentally or hypothesized in the literature to occur during dehydration, including leaf and internal tissue shrinkage, cell wall shrinkage, reduction in cell connectivity, and decreases in membrane permeability (Sancho-Knapik et al., 2011; Shatil-Cohen et al., 2011; Pou et al., 2013; Scoffoni et al., 2014; Sade et al., 2015), and with or without assuming an apoplastic barrier at the bundle sheath, as has been reported for some species (Lersten, 1997; Taneda et al., 2016). Across all four species, a reduction of membrane permeability in the context of an apoplastic barrier was the only factor that could directly account for the decline of K_{ox} values during dehydration. Model simulations showed that an 80% reduction in membrane permeability in the context of an apoplastic barrier resulted in a 58% to 86% decline of K_{ox} values. However, without an apoplastic barrier, the decrease of K_{ox} due to membrane permeability reduction would not be important enough to overcome the opposing effect of tissue shrinkage. Notably, leaf and tissue shrinkage as measured from microCT images (Fig. 5) would, by itself, actually increase K_{ox} by 4% to 55% across species, by shortening flow pathways outside the xylem (Fig. 6). Furthermore, an 80% reduction in cell connectivity had little impact, and in most cases (especially under the "no apoplastic barrier" scenario), its decrease was not sufficient to overcome the increase in K_{ox} induced by cell shrinkage (Fig. 6). Notably, an 80% reduction in cell wall thickness yielded reductions in K_{ox} regardless of simulating an apoplastic barrier or not, with 11% to 72% declines in K_{ox} at the turgor loss point across species and scenarios.

Table III. *Percentages of increase in leaf hydraulic resistance ($1/K_{leaf}$) contributed by increases in xylem resistance ($1/K_x$) and outside-xylem resistance ($1/K_{ox}$) at turgor loss point (TLP) and at the water potential at which K_{leaf} declined by 50% (P_{50}) and by 88% (P_{88})*

Species	Percentage Influence on K_{leaf} Decline at TLP		Percentage Influence on K_{leaf} Decline at Leaf P_{50}		Percentage Influence on K_{leaf} Decline at Leaf P_{88}	
	K_x	K_{ox}	K_x	K_{ox}	K_x	K_{ox}
C. betuloides	9.4	90.6	5.1	94.9	8.2	91.8
C. diversifolia	1.1	98.9	1.1	98.9	0.7	99.3
H. canariensis	2.2	97.8	0.9	99.1	1.4	98.6
L. camara	14.3	85.7	2.9	97.1	24.8	75.2
M. grandiflora	0.7	99.3	0.1	99.9	9.7	90.3
M. laurina	0.9	99.1	2.4	97.5	2.9	97.1
Q. agrifolia	0	100	0	100	0.2	99.8
S. canariensis	4.7	95.3	0.7	99.2	8.0	92.0

DISCUSSION

Vulnerable Outside-Xylem Pathways Protect the Xylem from Embolism throughout the Plant

Our results from both microCT imaging and hydraulics experiments suggest that the primary determinant of K_{leaf} decline in leaves from mild to extreme dehydration originated in vulnerability of the outside-xylem pathways and not hydraulic failure of the xylem. Across species, the decline in K_{ox} caused more than 85% of the decline in K_{leaf} by the turgor loss point and more than 75% by $P_{88,Kleaf}$. These results are consistent with the body of literature linking changes in aquaporin expression to leaf hydration status and bundle sheath and mesophyll cell turgor (see below; Johansson et al., 1998; Kim and Steudle, 2007, 2009; Miyazawa et al., 2008; Shatil-Cohen et al., 2011; Shatil-Cohen and Moshelion, 2012; Pou et al., 2013; Prado and Maurel, 2013; Laur and Hacke, 2014; Scoffoni et al., 2014; Sade et al., 2015). Our results are also consistent with those of two recent studies using an optical transmission approach, which found that long dehydrating times (up to 70 h)

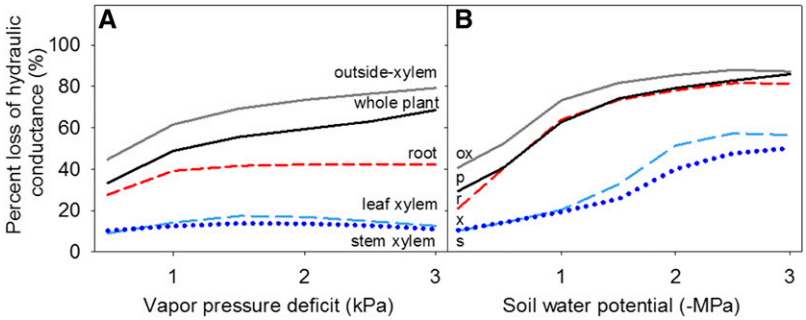

Figure 4. Model simulations of whole-plant hydraulic response to atmospheric drought (increasing vapor pressure deficit [VPD]; A) and dehydrating soil (B). Percentage loss of hydraulic conductance values plotted in both graphs are averages of simulations obtained for the four species tested (see "Materials and Methods"). The percentage loss of hydraulic conductance outside the xylem (ox; gray solid lines) is the main determinant of the decline of whole-plant hydraulic conductance (p; black solid lines) under both scenarios. Neither leaf xylem hydraulic conductance (x; dashed light blue lines) nor stem xylem hydraulic conductance (s; dotted dark blue lines) experiences strong declines with increasing soil drought or VPD. The root hydraulic conductance (dashed red lines) declines strongly under increasing soil drought and to a smaller extent under increasing VPD. Because the model simulates a transpiring plant, when the soil water potential is at zero on the *x* axis, the transpiring leaf water potential is still substantially negative, driving the decline of K_{leaf} from its maximum value (although not of K_x; for water potentials of each compartment, see Supplemental Table S2). Under the soil drought scenario, VPD was maintained at 0.5 kPa. Under the atmospheric drought scenario, soil water potential was maintained at −0.1 MPa.

and very negative water potentials below the turgor loss point were necessary before vein embolisms were observed in leaf veins (Brodribb et al., 2016a, 2016b). One of those studies showed a correlation between vein embolism and K_{leaf} decline in four species (Brodribb et al., 2016b), although this was not necessarily causative, as K_{leaf} appeared to decline by up to 50% before the turgor loss point and before any signal of embolism in leaf veins. Additionally, the sensitivity of K_{ox} and K_{leaf} may have been stronger under high irradiance. In that study, leaves were acclimated under low irradiance (less than 100 μmol quanta m^{-2} s^{-1}). For many species, K_{leaf} in hydrated leaves can be enhanced by many fold under high irradiance likely due to aquaporin expression (Cochard et al., 2007; Scoffoni et al., 2008; Maurel et al., 2015) and such high-light-acclimated leaves show stronger vulnerability before the turgor loss point (Guyot et al., 2012; Sack et al., 2016b). Similarly, a recent study partitioning the vulnerabilities of K_x and K_{ox} found that K_{ox} was the strongest determinant of K_{leaf} decline in two of four species (Trifiló et al., 2016), and, for the other two species, both xylem and outside-xylem pathways appeared to be strong drivers of K_{leaf} decline. However, hydraulics measurements were performed in that study under low light, likely minimizing the response of K_{ox} before the turgor loss point.

Our results for angiosperm leaves with their complex venation may be general for a yet greater diversity of plants, as two recent studies using microCT on needles of *Pinus pinaster* found few embolized conduits at needle water potentials that induced strong declines in K_{leaf} (Charra-Vaskou et al., 2012; Bouche et al., 2016).

These findings suggest that the leaf outside-xylem pathways, in addition to experiencing the most negative water potentials in the plant, also have very strong hydraulic vulnerability. Such results are consistent with the hypothesis that strong K_{ox} declines would act as a protective bottleneck, shielding the leaf and stem xylem under many scenarios of atmospheric and soil drought from tensions that would induce catastrophic embolisms (Scoffoni et al., 2014). Additional mechanisms for protection may operate; a recent study found that minor vein collapse in leaves of red oak (*Quercus rubra*) occurred under very strong tensions below the turgor loss point (more negative than −3 MPa) and, thus, could act as a further buffer against embolism under prolonged drought (Zhang et al., 2016). Notably, a similar protection occurs in roots, as cortical lacunae formation in fine roots induced strong declines in hydraulic conductance protecting root xylem conduits from embolism formation (Cuneo et al., 2016). Such a strong role of outside-xylem pathways in hydraulic decline in both leaves and roots suggests a general advantage throughout the plant of sensitive living tissues protecting the xylem from catastrophic embolism. Given that stem embolism may be in many or most cases irreversible (Urli et al., 2013), such a protective effect would be most important for long-lived leaves and stems with high carbon investment, as commonly found in many drought-prone systems such as chaparral communities. This hypothesis of the importance of the K_{ox} response was supported by our model simulations showing that whole-plant hydraulic conductance would decline under increasing soil drought and/or atmospheric drought (i.e. high VPD) primarily as a consequence of the strong declines in K_{ox}. Because the leaves experience the lowest water potentials, and declining K_{ox} provides an increasing bottleneck in the system, the tensions developed in leaf and stem xylem were, in most modeled scenarios, insufficient

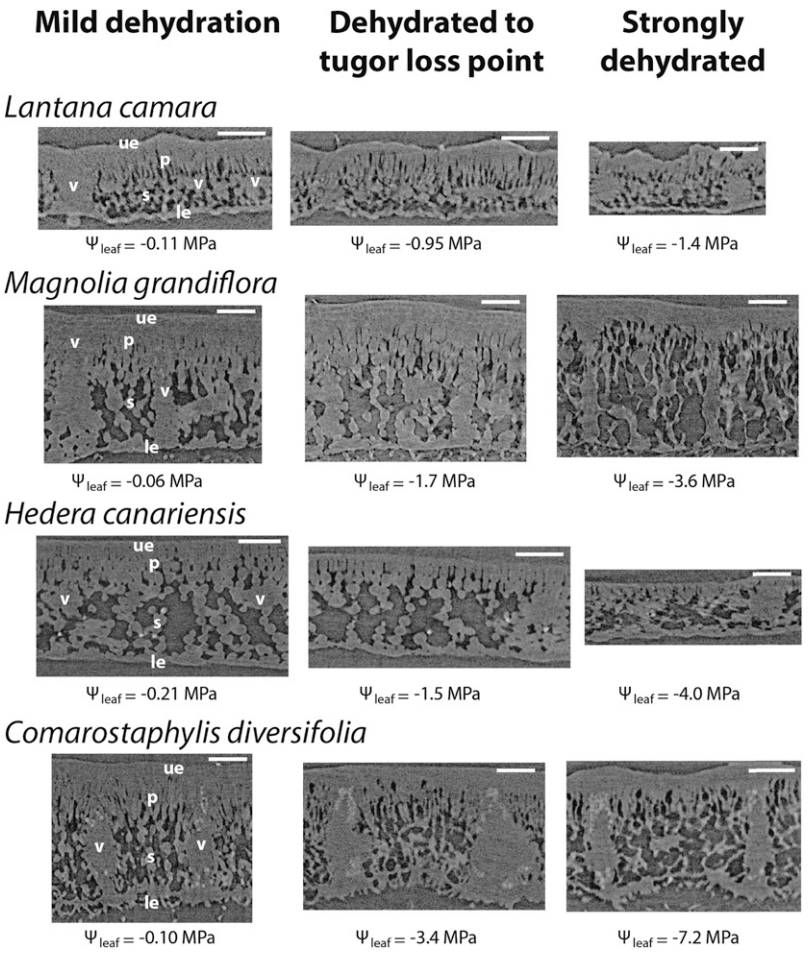

Figure 5. MicroCT scans of leaf laminas at three dehydration levels for four species. Symbols are as follows: leaf water potential (Ψ_{leaf}), vascular bundle (v), spongy mesophyll cell (s), palisade mesophyll cell (p), upper epidermal cell (ue), and lower epidermal cell (le). Bars = 250 μm.

to cause catastrophic embolism. The declines in K_{ox} and K_{leaf} may further protect the stem xylem from strong tensions and embolism if the strongly declining water potentials in the mesophyll influence stomatal closure, which tends to begin well above Ψ_{TLP} (Bartlett et al., 2016), and K_{ox} could play an important role in stomatal control. Another potential advantage of outside-xylem pathways being more sensitive to dehydration is that they might recover more rapidly with water potential than embolized conduits in the xylem. Thus, changes in outside-xylem pathways with dehydration could be more reversible during drought and recovery cycles than xylem embolism. While xylem embolism requires several hours under no tension to recover by capillarity (Hochberg et al., 2016; Knipfer et al., 2016), in some species, K_{leaf} can partially recover after only 1 h of rehydration (Scoffoni et al., 2012), which could be due to the recovery of K_{ox}. Future work should resolve the influence of K_x and K_{ox} decline on stomatal conductance and their recovery.

These results provide strong evidence for the role of outside-xylem pathways in driving changes in K_{leaf} and whole-plant conductance under the range of water potentials that plants experience through mild and moderate drought stress. In contrast, after stomatal closure and under conditions of prolonged drought, sustained dehydration will induce embolism in leaf veins and, likely, in the stem xylem, eventually contributing to hydraulic failure and plant death (Anderegg et al., 2015).

Determinants of K_{ox} Decline with Dehydration

Given the key role of K_{ox} decline in dehydrating leaves, resolving the underlying causes is crucial. Experimental investigation remains challenging not only because of the complexity of liquid water movement through the living tissues outside the vein xylem but also because vapor-phase pathways contribute to K_{ox} and thus K_{leaf} (Pieruschka et al., 2010; Rockwell et al., 2014; Buckley et al., 2015). We implemented a spatially explicit model for the anatomical and biophysical determination of K_{ox} (MOFLO; Buckley et al., 2015) and parameterized the model with our measurements of tissue structure in dehydrating leaves. These simulations showed that shrinking cells and air spaces in dehydrating leaves would in fact act to increase K_{ox} due to the effects of shorter path lengths for water transport

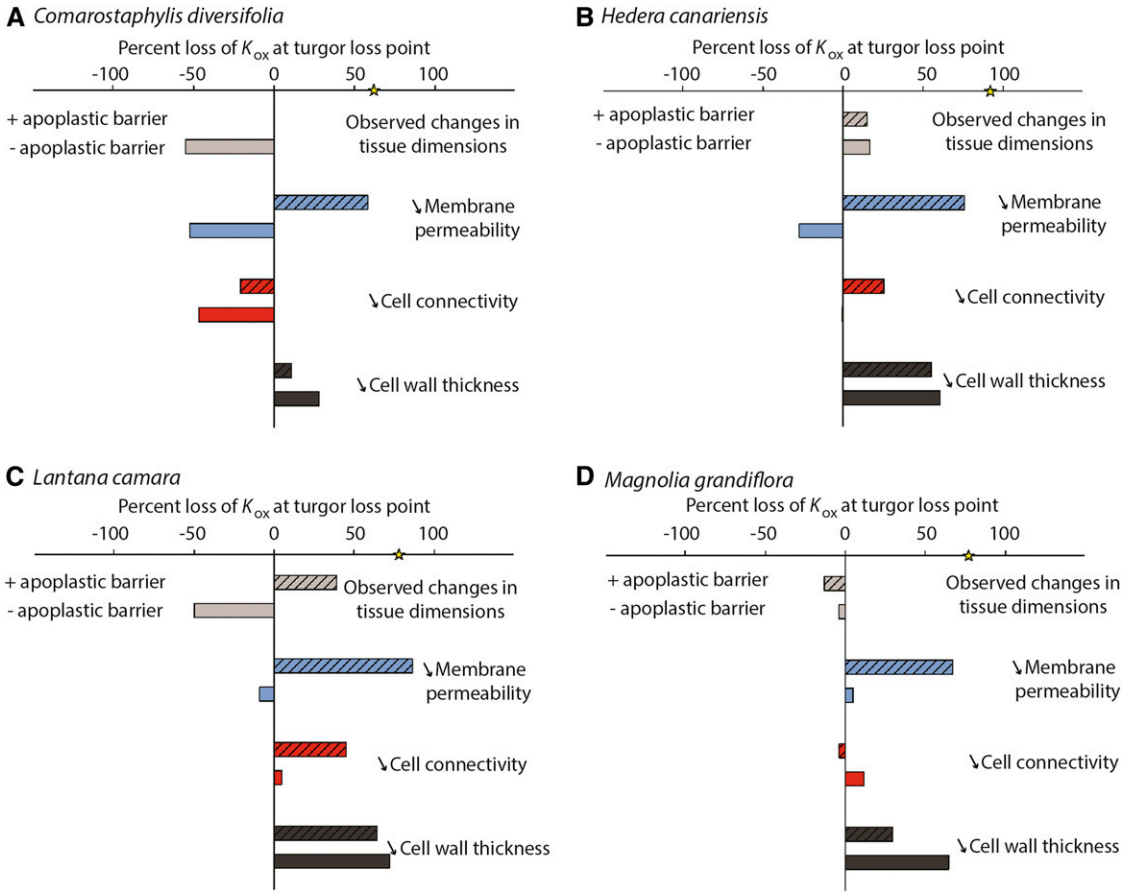

Figure 6. Testing hypotheses for the potential drivers of the decline in K_{ox} in dehydrating leaves, using a spatially explicit model of leaf outside-xylem water transport (see "Materials and Methods"). Parameterizing the model for four species, we estimated the K_{ox} based on the decline of observed cell size, porosity (air space), and leaf area at the turgor loss point (light gray bars). Because in some cases these changes in tissue dimensions resulted in an increase in K_{ox}, we modeled K_{ox} decline according to three scenarios (always including the observed changes in tissue dimension): an 80% decline at the turgor loss point in membrane permeability (blue bars), cell connectivity (red bars), and cell wall thickness (dark gray bars). All simulations were run with or without an apoplastic barrier at the bundle sheath cells (solid versus striped bars). The yellow star on the *x* axis represents the observed percentage K_{ox} decline at the turgor loss point. Across all four species, only simulations of a strong decrease in membrane permeability in leaves with an apoplastic barrier could explain the observed declines in K_{ox}.

to the stomata, both horizontally, as effective vein length per leaf area increases, and vertically, from vein to stomata, given the shrinkage of the leaf thickness. Simulations showed that declines in membrane permeability could be important determinants of K_{ox} decline that would drive K_{leaf} decline overall, despite the effect of reduced tissue dimensions. A decline in membrane permeability could result from reduced aquaporin activity as cells dehydrate, a response demonstrated previously in studies using mutants of the model species Arabidopsis (*Arabidopsis thaliana*) and in cell probe studies of maize (*Zea mays*; Johansson et al., 1998; Kim and Steudle, 2007; Maurel et al., 2015). Furthermore, previous studies have found that aquaporin mutants and leaves of species previously perfused with aquaporin inhibitors to exhibit up to a 75% decrease of K_{leaf} (Shatil-Cohen et al., 2011; Pou et al., 2013; Sade et al., 2015). Our findings are in line with the hypothesis that reduced aquaporin activity, potentially triggered by turgor decline and/or abscisic acid production during dehydration, would drive K_{ox} decline (Shatil-Cohen et al., 2011) and further suggest that such a response would scale up to determine the decline of K_{leaf} and whole-plant hydraulic decline. We found that, to model the observed declines of K_{ox} due to the reduction of membrane permeability, it was necessary to posit an apoplastic barrier at the bundle sheath, analogous to the Casparian strip in root endodermis (Canny, 1986, 1988), to constrain all water to exit the veins via bundle sheath cell membranes rather than via the apoplast. Such an apoplastic barrier has been supported previously by dye experiments (Shatil-Cohen et al., 2011; Shatil-Cohen and Moshelion, 2012) and hydraulics measurements in other species (Sack et al., 2004; Sade et al., 2014) and visualized in anatomical studies of some, but not all, species tested (Canny, 1986;

Lersten, 1997; Wu et al., 2005; Ribeiro et al., 2007; Taneda et al., 2016). The restriction of water movement needed to explain declines in K_{ox} could occur at the site at which water exits the vascular parenchyma to reach bundle sheath cells or cell walls or via a forced symplastic flow path through the vascular parenchyma cells until it reaches the bundle sheath; any of these mechanisms would strongly increase the resistance in water movement (Buckley, 2015). Elucidating whether such apoplastic barriers or symplastic flows through vascular parenchyma are typical is an important topic for future studies. Finally, modeling showed that changes in cell wall thickness during dehydration could strongly influence K_{ox} (Fig. 6), given the important contribution of apoplastic cell wall pathways through the mesophyll in determining K_{ox} at full hydration (Buckley, 2015). However, to our knowledge, such putative changes in cell wall thickness with dehydration have never been documented. Our results, along with the numerous aquaporin studies (see refs. above), most strongly support changes in membrane permeability at the vascular parenchyma or bundle sheath cell level as a mechanism for the decline in K_{ox} with dehydration.

K_{ox} Vulnerability in Relation to Dought Tolerance

Across species, K_{ox} and K_x vulnerability during leaf dehydration correlated strongly with Ψ_{TLP}. Ψ_{TLP} is a good indicator of species drought tolerance across ecosystems, with more negative values present in species occurring in drier habitats or ecosystems (Bartlett et al., 2012). Recently, several studies have shown strong correlation of $P_{50,Kleaf}$ with Ψ_{TLP} across diverse angiosperm species (Blackman et al., 2010; Scoffoni et al., 2012). These studies hypothesized that cells maintaining turgor at more negative water potentials could preserve cell integrity and, thus, hydraulic pathways outside the xylem and, therefore, confer resistance to hydraulic decline. However, given that our model simulations revealed that cell shrinkage would not cause a decline in K_{ox} as hypothesized previously (Scoffoni et al., 2014), an indirect mechanism must underlie this correlation; for instance, a more negative Ψ_{TLP} may correspond to a greater ability to maintain cell membrane permeability, especially in the vascular parenchyma and/or bundle sheath (Kim and Steudle, 2007). The hypothesis that cell turgor loss might trigger aquaporin deactivation and/or abscisic acid production (Pierce and Raschke, 1980; Shatil-Cohen et al., 2011), which in turn would reduce membrane permeability, is consistent with recent work on cells and tissues in a range of species (Wan et al., 2004; Ye et al., 2005; Kim and Steudle, 2007; Shatil-Cohen et al., 2011; Brodribb and McAdam, 2013; Chaumont and Tyerman, 2014; McAdam and Brodribb, 2014; Vandeleur et al., 2014). Another source of the coordination of Ψ_{TLP} with the hydraulic vulnerability of the leaf and its compartments is that all of these physiologically important traits are coselected in species with greater drought tolerance (Blackman et al., 2010, 2014; Bartlett et al., 2012, 2016).

CONCLUSION

Combining empirical, visual, and modeling approaches, we found that, in eight diverse species, the observed decline in K_{leaf} during mild dehydration results primarily from losses in hydraulic conductance outside the vascular system (more than 75% across leaf dehydration from mild to extreme; 96% on average). These results indicate that outside-xylem processes are the main determinants of K_{leaf} vulnerability to dehydration. Leaves avoid catastrophic xylem failure by regulating their K_{ox}. After stomatal closure and under extreme drought, leaf vein and stem embolism might be unavoidable and induce catastrophic hydraulic failure. These findings pinpoint the mesophyll tissues, including the bundle sheath, as a central locus for the control of leaf and plant water transport during progressive drought.

MATERIALS AND METHODS

Plant Material

Measurements were obtained for eight species diverse in phylogeny, origin, drought tolerance, and life form (Table I), growing in and around the campus of the University of California, Los Angeles, and Will Rogers State Park. Measurements were conducted from November 2013 to November 2014. The day before any of the measurements described below, shoots with a minimum of three nodes of stem below the leaves to be studied were excised in air from at least three individuals and transported in dark plastic bags filled with wet paper towels, where the shoot was recut underwater by a minimum of two nodes from the base and left to rehydrate overnight. We note that, although obtained in different years, both leaf and xylem hydraulic vulnerability curves were obtained from the same individuals, and no differences were found in K_{leaf} values across years (Scoffoni et al., 2011; Guyot et al., 2012).

MicroCT

To directly visualize embolism in the xylem and structural changes in all orders of veins and in the mesophyll tissues, we used high-energy, high-resolution microCT at the synchrotron at the Advanced Light Source in Berkeley, California (Beamline 8.3.2), in November 2014. Stacks of images were obtained by scanning the center (including the midvein) of living leaves on dehydrating shoots for four of our study species (*Comarostaphylis diversifolia*, *Hedera canariensis*, *Lantana camara*, and *Magnolia grandiflora*). Species were chosen for microCT based on their wide range of drought tolerance. A detailed description of sample preparation for microCT imaging is given in Supplemental Materials and Methods S1. Nine to 12 scans of the midrib and surrounding mesophyll at the center of the leaf were made per species of leaves spanning the whole range of leaf water potential obtained in the K_x vulnerability curves (described below).

On three cross-sectional images randomly selected at the bottom, middle, and top part along the main axis of the microCT scan, conduit embolism in the midrib, along with mesophyll cell and tissue dimensions, were quantified. For each image, we measured the number of embolized conduits in the midrib and averaged for three areas of the leaf lamina measurements of the dimensions of tissues and cells (epidermis and cuticle, palisade mesophyll, spongy mesophyll, and palisade cell area, height, and diameter) using ImageJ software (version 1.46r; National Institutes of Health). Bundle sheath thickness and cell dimensions could not be resolved in these images. Three-dimensional volume renderings of our scans were made using Avizo 8.1.1 software (VSG) and used to

determine the vein orders (identified by following the branching pattern from the secondary veins), and cross-sectional images at the start, middle, and end of the scanned region were used to determine the number of embolized conduits.

We calculated the %EMC at given leaf water potentials. Embolized conduits appear brightly in the images, but nonembolized conduits cannot be distinguished from each other or counted. Thus, we estimated the total number of midrib conduits in cross sections of these leaves using data taken from cross sections of three leaves sampled from the same plants of each species and visualized by light microscopy (Supplemental Fig. S3; for methods, see "Light Microscopy of Cells and Tissues within Leaves" below). Given that the number of midrib xylem conduits scales with the midrib vascular cross-sectional area for well-hydrated leaves of given species (Coomes et al., 2008; Taneda and Terashima, 2012), we counted the total number of xylem conduits in the midrib cross sections obtained from light microscopy for hydrated leaves and normalized by their midrib vascular area. These were averaged for each species to determine the conduit number per vascular area for hydrated leaves (CNA_{hydr}). Cross sections for both light microscopy and microCT scans were taken at the leaf midrib center. To calculate the total number of midrib conduits in cross sections of the scanned dehydrated leaves (CN), we had to account for the shrinkage of the midrib vascular area with water potential. For the scanned dehydrated leaves of each species, we plotted midrib vascular area for the dehydrated leaves (A_{dehyr}) and for the three fully hydrated leaves measured using light microscopy against leaf water potential (Supplemental Fig. S4) and thus estimated the proportion of area shrinkage relative to the value extrapolated to 0 MPa for each leaf (AS_{dehydr}). The conduit number (CN) for each individual scanned leaf was obtained as:

$$CN = CNA_{hydr} \times \frac{A_{dehydr}}{(1 - AS_{dehydr})} \quad (2)$$

We counted the number of embolized conduits in each scanned leaf (CN_{emb}) and calculated % EMC as:

$$\%\ EMC = \frac{CN_{emb}}{CN} \times 100 \quad (3)$$

We note that the %EMC values differ slightly from those reported previously for the same images (Scoffoni et al., 2017), as we improved the calculation by adding the areas of the three light microscopy images of fully hydrated leaves to the regression against water potential to determine AS_{dehydr}. This improved calculation resulted in no major changes in the patterns observed.

We considered the potential concern that the x-ray beam might produce damage artifacts that might have contributed uncertainty to the interpretation of the images. However, no damage from the x-ray beam was observed in our samples. Only a few gas-filled conduits were found at high water potentials in two species, which was to be expected given our sampling design (i.e. excising small shoots in air), as a small portion of conduits originating in the stem would extend into the leaf (Scoffoni and Sack, 2015). Another indication that microCT faithfully represents mesophyll structure is that cell dimensions measured in the microCT scan images for hydrated leaves were statistically similar to those made on fully hydrated leaves of the same species using light microscopy (repeated-measures ANOVA was performed in Minitab 16; results are given in Supplemental Table S3).

Measuring Leaf and Leaf Xylem Hydraulic Vulnerability Curves

Leaf hydraulic vulnerability curves for seven of the eight study species were published previously for the same individuals used in this study (Scoffoni et al., 2011; Scoffoni and Sack, 2015), and that for *Malosma laurina* was constructed for this study. Measurements of K_{leaf} vulnerability were made using the evaporative flux method (Supplemental Materials and Methods S1; Sack et al., 2002; Scoffoni et al., 2012), for which detailed protocols are available (Sack and Scoffoni, 2012). All measurements were performed on leaves acclimated to high light for over 30 min (greater than 1,000 μmol photons $m^{-2}\,s^{-1}$). We constructed K_x vulnerability curves using the vacuum pump method (Supplemental Materials and Methods S1) for the same individuals and species from which K_{leaf} vulnerability curves were obtained. Data for four species (i.e. *Comarostaphylis diversifolia*, *Hedera canariensis*, *Quercus agrifolia*, and *Salvia canariensis*) were published previously in a study of potential methodological artifacts in leaf hydraulic measurements (Scoffoni and Sack, 2015), and additional measurements were made here for four other species (*Cercocarpus betuloides*, *Lantana camara*, *Magnolia grandiflora*, and *M. laurina*).

To construct hydraulic vulnerability curves, we selected the maximum likelihood function that best fitted data for each species using the optim function in R 3.1.0 (http://www.r-project.org; Burnham and Anderson, 2004; Scoffoni et al., 2012). Five functions were tested according to previous studies (Pammenter and Vander Willigen, 1998; Scoffoni et al., 2012): a linear function ($K_z = a\Psi_z + b$), a two-parameter sigmoidal function ($K_z = \frac{100}{1 + e^{(a(\Psi_z - b))}}$), a three-parameter sigmoidal function ($K_z = \frac{a}{1 + e^{-\left(\frac{\Psi_z - x_0}{b}\right)}}$), a logistic function ($K_z = \frac{a}{1 + \left(\frac{\Psi_z}{x_0}\right)^b}$), and an exponential function ($K_z = y_0 + ae^{-b\Psi_z}$). The K_z and Ψ_z in the above functions represent either the K_{leaf} or K_x and water potentials. Functions were compared using the Akaike Information Criterion (AIC) corrected for low n. The function with the lowest AIC value (differences of greater than 2 considered) was chosen as the maximum likelihood function.

Determination of Leaf Outside-Xylem Vulnerability Curves

Based on Equation 1, we constructed K_{ox} vulnerability curves from K_{leaf} and K_x values along the water potential range tested for given species (i.e. from maximum K_{leaf} until it had declined to a negligible level). Thus, for the different water potentials, each K_{ox} point was obtained as the reciprocal of the difference between K_{leaf}^{-1} and K_x^{-1} following Equation 1. For background and justification of this subtraction method, see Supplemental Materials and Methods S1.

Whole-Plant Hydraulic Model Simulations

We modeled the influence of leaf hydraulic declines on the plant hydraulic system under simulated soil and atmospheric drought using a previously described approach (Osborne and Sack, 2012). The plant hydraulic stomatal model is based on Darcy's law, assumes steady-state flow, and simultaneously resolves water potentials and hydraulic conductance for each plant component, given inputs of soil water potential and VPD and parameters for the response of the hydraulic conductance of whole root, whole stem, leaf xylem and outside xylem, and stomatal conductance to water potential within the respective organ. For the four species tested, we simulated the impact of declining soil water potential or increasing VPD given the measured vulnerability curves for K_{ox} and K_x, obtained as described above. We did not have data for the response of the stem, root, or stomata to dehydration for these species, so we used estimates based on current understanding in the literature. Thus, we assumed the vulnerability curve of the whole-stem xylem to follow a sigmoid pattern, with maximum hydraulic conductance representing half of the whole-plant resistance (Tyree and Zimmermann, 2002). To be conservative, we assigned to the stem a water potential at 50% loss of hydraulic conductance equal to that of the leaf xylem, since xylem conduits in the stem are expected to undergo air seeding at similar or more negative water potentials (Tyree and Ewers, 1991; Choat et al., 2005). Thus, the stem xylem was modeled as potentially more sensitive than it might be in reality, making more robust our finding of its low hydraulic decline when the whole plant is droughted, due to the role of leaf hydraulic decline in minimizing tensions in the stem. We assumed the root vulnerability curve to be equal to the whole-leaf hydraulic vulnerability curve (obtained as described above), given that, on average, the root and leaf contribute approximately the same resistance throughout the whole plant (Tyree and Zimmermann, 2002) and have both xylem and extraxylem pathways for water movement (Tyree and Zimmermann, 2002). We set the stomatal conductance decline with leaf water potential as similar to that of the vulnerability of the leaf outside-xylem pathways, using a maximum stomatal conductance value of 300 mmol $m^{-2}\,s^{-1}$ across species. A range of alternative parameterizations did not change the overall findings (data not shown). We note that future work will enable more precise calibration of the model (e.g. with vulnerability functions for all organs). Simulations were run in Python 2.7.10 using the future, scipy, and pandas packages. Model code is available on request.

Modeling the Outside-Xylem Flow Pathways with Dehydration

We used a spatially explicit model of outside-xylem flow pathways in the leaf (MOFLO; Buckley et al., 2015) that can be parameterized with leaf anatomy to investigate potential causes of the strong declines in K_{ox} observed with dehydration. We first simulated the impact of anatomical changes alone, based on anatomical measurements at different water potentials, including epidermal, spongy, and palisade mesophyll cell shrinkage (obtained from micro-CT

images as described above; Fig. 5), percentage leaf area shrinkage (which influences vein length per leaf area), and percentage intercellular air space change (published previously for these same species and individuals; Scoffoni et al., 2014). Since bundle sheath cell area could not be determined in the micro-CT images, we assumed that these cells shrank by the same percentage as spongy mesophyll cells. We then simulated the impact on K_{ox} of the decline in membrane permeability, cell connectivity, and cell wall thickness at the turgor loss point, using values for tissue dimensions observed at the turgor loss point. Given that we did not have measurements of membrane permeability, cell connectivity, and cell wall thickness at the turgor loss point, we estimated the reduction in these parameters required to cause the observed decline in K_{ox} at the turgor loss point. We repeated all of these simulations under two scenarios: with and without an apoplastic barrier at the bundle sheath cells.

Measurement of the Turgor Loss Point

The leaf turgor loss point for seven of eight species was obtained from pressure-volume curves of previously published studies (Scoffoni et al., 2012, 2014) that were based on the same individuals of the study species. Pressure-volume curves were obtained for five leaves of three individuals of *M. laurina* in the fall of 2014 using a detailed published standard protocol (Sack, 2010).

Light Microscopy of Cells and Tissues within Leaves

For measurements of leaf cross-sectional anatomy, we used images from a previously published study of different anatomical traits made on the same individuals of four study species (John et al., 2013). Briefly, from each leaf center, a 1- × 0.5-cm rectangle was cut and embedded gradually in low-viscosity acrylic resin (L.R. White; London Resin) in ethanol, under vacuum over the course of 1 week, then dried at 55°C overnight. Samples were then sectioned using glass knives (cut using an LKB 7800 KnifeMaker; LKB Produkter) at 1 μm thickness in a rotary microtome (Leica Ultracut E; Reichter-Jung). Sections were stained in 0.01% Toluidine Blue in 1% sodium borate and imaged using 5×, 10×, 20×, and 40× objectives using a light microscope (Leica Lietz DMRB; Leica Microsystems) with a camera utilizing SPOT advanced imaging software (SPOT Imaging Solutions; Diagnostic Instruments) for a total image magnification of 287× to 2,300×. Using ImageJ, we measured the vascular bundle area in the midrib and counted the total number of xylem conduits.

Statistics

To test the causal influences of xylem and outside-xylem conductance decline on whole-leaf hydraulic decline, we used three analyses. First, we calculated causal effects within species by partitioning changes in leaf resistance ($R_{leaf} = 1/K_{leaf}$) into changes in xylem resistance ($R_x = 1/K_x$) and outside-xylem resistance ($R_x = 1/K_{ox}$); since $R_{leaf} = R_x + R_{ox}$, $\Delta R_{leaf} = \Delta R_x + \Delta R_{ox}$, where Δ denotes a change between full turgor and either the turgor loss point or P_{50}. Thus, for example, the percentage of leaf hydraulic decline due to outside-xylem pathways was calculated as $\Delta R_{ox}/\Delta R_{leaf} \times 100\%$. Then, we estimated the importance of K_x and K_{ox} decline in explaining species differences in leaf hydraulic vulnerability (i.e. in $P_{50,Kleaf}$). We tested whether $P_{50,Kleaf}$ was best predicted by the water potential at 50% decline in xylem hydraulic conductance ($P_{50,Kx}$) or that of outside-xylem hydraulic conductance ($P_{50,Kox}$), or their combined effect, according to the following models: $P_{50,Kleaf} = a+bP_{50,Kx}$, $P_{50,Kleaf} = a+bP_{50,Kox}$, or $P_{50,Kleaf} = a+bP_{50,Kox} + cP_{50,Kx}$. We used maximum likelihood selection of the best model using the optim function in R 3.1.0 (Burnham and Anderson, 2004; Scoffoni et al., 2012). The model with the lowest AIC corrected for low n by at least 2 was selected as the maximum likelihood model. We also applied independent effects analysis, which is suited to robustly determine the contribution of correlated predictor variables to an output variable (Murray and Conner, 2009), and thereby calculated the percentage contribution of $P_{50,Kx}$ and $P_{50,Kox}$ to the variation across species in $P_{50,Kleaf}$, using the hier.part function in R.3.1.0.

Supplemental Data

The following supplemental materials are available.

Supplemental Figure S1. Decline of leaf K_x with dehydration.

Supplemental Figure S2. Model simulations of plant hydraulic response to dehydrating soil and increasing VPD for four diverse species.

Supplemental Figure S3. Light microscopy midrib cross sections of the four study species used for microCT.

Supplemental Figure S4. Percentage midrib vascular area of maximum at full hydration plotted against leaf water potential.

Supplemental Table S1. Parameters for the three models tested to best predict $P_{50,Kleaf}$.

Supplemental Table S2. Inputs and results for the whole-plant hydraulic model simulations.

Supplemental Table S3. Means ± SE of cell dimensions measured from microCT scans and light microscopy.

Supplemental Materials and Methods S1.

ACKNOWLEDGMENTS

We thank the Advanced Light Source in Berkeley, California (Beamline 8.3.2), Dula Parkinson for technical assistance, and Steven Jansen for helpful discussion and comments on the article.

Received October 24, 2016; accepted December 28, 2016; published January 3, 2017.

LITERATURE CITED

Anderegg WRL, Flint A, Huang C, Flint L, Berry JA, Davis FW, Sperry JS, Field CB (2015) Tree mortality predicted from drought-induced vascular damage. Nat Geosci **8:** 367–371

Bartlett MK, Klein T, Jansen S, Choat B, Sack L (2016) The correlations and sequence of plant stomatal, hydraulic, and wilting responses to drought. Proc Natl Acad Sci USA **113:** 13098–13103

Bartlett MK, Scoffoni C, Sack L (2012) The determinants of leaf turgor loss point and prediction of drought tolerance of species and biomes: a global meta-analysis. Ecol Lett **15:** 393–405

Blackman CJ, Brodribb TJ, Jordan GJ (2010) Leaf hydraulic vulnerability is related to conduit dimensions and drought resistance across a diverse range of woody angiosperms. New Phytol **188:** 1113–1123

Blackman CJ, Gleason SM, Chang Y, Cook AM, Laws C, Westoby M (2014) Leaf hydraulic vulnerability to drought is linked to site water availability across a broad range of species and climates. Ann Bot (Lond) **114:** 435–440

Bouche PS, Delzon S, Choat B, Badel E, Brodribb TJ, Burlett R, Cochard H, Charra-Vaskou K, Lavigne B, Li S, et al (2016) Are needles of Pinus pinaster more vulnerable to xylem embolism than branches? New insights from x-ray computed tomography. Plant Cell Environ **39:** 860–870

Boyer JS (1985) Water transport. Annu Rev Plant Physiol **36:** 473–516

Brodribb TJ, Bienaimé D, Marmottant P (2016a) Revealing catastrophic failure of leaf networks under stress. Proc Natl Acad Sci USA **113:** 4865–4869

Brodribb TJ, Hill RS (2000) Increases in water potential gradient reduce xylem conductivity in whole plants: evidence from a low-pressure conductivity method. Plant Physiol **123:** 1021–1027

Brodribb TJ, Holbrook NM (2003) Stomatal closure during leaf dehydration, correlation with other leaf physiological traits. Plant Physiol **132:** 2166–2173

Brodribb TJ, Holbrook NM (2005) Water stress deforms tracheids peripheral to the leaf vein of a tropical conifer. Plant Physiol **137:** 1139–1146

Brodribb TJ, Holbrook NM (2006) Declining hydraulic efficiency as transpiring leaves desiccate: two types of response. Plant Cell Environ **29:** 2205–2215

Brodribb TJ, McAdam SAM (2013) Abscisic acid mediates a divergence in the drought response of two conifers. Plant Physiol **162:** 1370–1377

Brodribb TJ, Skelton RP, McAdam SAM, Bienaimé D, Lucani CJ, Marmottant P (2016b) Visual quantification of embolism reveals leaf vulnerability to hydraulic failure. New Phytol **209:** 1403–1409

Bucci SJ, Scholz FG, Goldstein G, Meinzer FC, Sternberg LDL (2003) Dynamic changes in hydraulic conductivity in petioles of two savanna tree species: factors and mechanisms contributing to the refilling of embolized vessels. Plant Cell Environ **26:** 1633–1645

Buckley TN (2015) The contributions of apoplastic, symplastic and gas phase pathways for water transport outside the bundle sheath in leaves. Plant Cell Environ **38:** 7–22

Buckley TN, John GP, Scoffoni C, Sack L (2015) How does leaf anatomy influence water transport outside the xylem? Plant Physiol **168:** 1616–1635

Burnham KP, Anderson DR (2004) Multimodel inference: understanding AIC and BIC in model selection. Sociol Methods Res **33:** 261–304

Canny MJ (1986) Water pathways in wheat leaves. 3. The passage of the mestome sheath and the function of the suberized lamellae. Physiol Plant **66:** 637–647

Canny MJ (1988) Water pathways in wheat leaves. 4. The interpretation of images of a fluorescent apoplastic tracer. Aust J Plant Physiol **15:** 541–555

Charra-Vaskou K, Badel E, Burlett R, Cochard H, Delzon S, Mayr S (2012) Hydraulic efficiency and safety of vascular and non-vascular components in Pinus pinaster leaves. Tree Physiol **32:** 1161–1170

Chaumont F, Tyerman SD (2014) Aquaporins: highly regulated channels controlling plant water relations. Plant Physiol **164:** 1600–1618

Choat B, Jansen S, Brodribb TJ, Cochard H, Delzon S, Bhaskar R, Bucci SJ, Feild TS, Gleason SM, Hacke UG, et al (2012) Global convergence in the vulnerability of forests to drought. Nature **491:** 752–755

Choat B, Lahr EC, Melcher P, Zwieniecki MA, Holbrook NM (2005) The spatial pattern of air seeding thresholds in mature sugar maple trees. Plant Cell Environ **28:** 1082–1089

Cochard H, Badel E, Herbette S, Delzon S, Choat B, Jansen S (2013) Methods for measuring plant vulnerability to cavitation: a critical review. J Exp Bot **64:** 4779–4791

Cochard H, Bodet C, Améglio T, Cruiziat P (2000) Cryo-scanning electron microscopy observations of vessel content during transpiration in walnut petioles: facts or artifacts? Plant Physiol **124:** 1191–1202

Cochard H, Venisse JS, Barigah TS, Brunel N, Herbette S, Guilliot A, Tyree MT, Sakr S (2007) Putative role of aquaporins in variable hydraulic conductance of leaves in response to light. Plant Physiol **143:** 122–133

Coomes DA, Heathcote S, Godfrey ER, Shepherd JJ, Sack L (2008) Scaling of xylem vessels and veins within the leaves of oak species. Biol Lett **4:** 302–306

Crombie DS, Milburn JA, Hipkins MF (1985) Maximum sustainable xylem sap tensions in *Rhododendron* and other species. Planta **163:** 27–33

Cuneo IF, Knipfer T, Brodersen CR, McElrone AJ (2016) Mechanical failure of fine root cortical cells initiates plant hydraulic decline during drought. Plant Physiol **172:** 1669–1678

Diffenbaugh NS, Swain DL, Touma D (2015) Anthropogenic warming has increased drought risk in California. Proc Natl Acad Sci USA **112:** 3931–3936

Dixon HH, Joly J (1895) On the ascent of sap. Philos Trans R Soc Lond **186:** 563–576

Guyot G, Scoffoni C, Sack L (2012) Combined impacts of irradiance and dehydration on leaf hydraulic conductance: insights into vulnerability and stomatal control. Plant Cell Environ **35:** 857–871

Hacke UG, Sperry JS, Pittermann J (2000) Drought experience and cavitation resistance in six shrubs from the Great Basin, Utah. Basic Appl Ecol **1:** 31–41

Hernandez-Santana V, Rodriguez-Dominguez CM, Fernández JE, Diaz-Espejo A (2016) Role of leaf hydraulic conductance in the regulation of stomatal conductance in almond and olive in response to water stress. Tree Physiol **36:** 725–735

Hochberg U, Albuquerque C, Rachmilevitch S, Cochard H, David-Schwartz R, Brodersen CR, McElrone A, Windt CW (2016) Grapevine petioles are more sensitive to drought induced embolism than stems: evidence from in vivo MRI and microcomputed tomography observations of hydraulic vulnerability segmentation. Plant Cell Environ **39:** 1886–1894

Johansson I, Karlsson M, Shukla VK, Chrispeels MJ, Larsson C, Kjellbom P (1998) Water transport activity of the plasma membrane aquaporin PM28A is regulated by phosphorylation. Plant Cell **10:** 451–459

John GP, Scoffoni C, Sack L (2013) Allometry of cells and tissues within leaves. Am J Bot **100:** 1936–1948

Johnson DM, McCulloh KA, Woodruff DR, Meinzer FC (2012) Evidence for xylem embolism as a primary factor in dehydration-induced declines in leaf hydraulic conductance. Plant Cell Environ **35:** 760–769

Johnson DM, Meinzer FC, Woodruff DR, McCulloh KA (2009a) Leaf xylem embolism, detected acoustically and by cryo-SEM, corresponds to decreases in leaf hydraulic conductance in four evergreen species. Plant Cell Environ **32:** 828–836

Johnson DM, Woodruff DR, McCulloh KA, Meinzer FC (2009b) Leaf hydraulic conductance, measured in situ, declines and recovers daily: leaf hydraulics, water potential and stomatal conductance in four temperate and three tropical tree species. Tree Physiol **29:** 879–887

Kikuta SB, LoGullo MA, Nardini A, Richter H, Salleo S (1997) Ultrasound acoustic emissions from dehydrating leaves of deciduous and evergreen trees. Plant Cell Environ **20:** 1381–1390

Kim YX, Steudle E (2007) Light and turgor affect the water permeability (aquaporins) of parenchyma cells in the midrib of leaves of *Zea mays*. J Exp Bot **58:** 4119–4129

Kim YX, Steudle E (2009) Gating of aquaporins by light and reactive oxygen species in leaf parenchyma cells of the midrib of *Zea mays*. J Exp Bot **60:** 547–556

Knipfer T, Cuneo IF, Brodersen CR, McElrone AJ (2016) In situ visualization of the dynamics in xylem embolism formation and removal in the absence of root pressure: a study on excised grapevine stems. Plant Physiol **171:** 1024–1036

Laur J, Hacke UG (2014) Exploring *Picea glauca* aquaporins in the context of needle water uptake and xylem refilling. New Phytol **203:** 388–400

Lersten NR (1997) Occurrence of endodermis with a Casparian strip in stem and leaf. Bot Rev **63:** 265–272

Lo Gullo MA, Nardini A, Trifilo P, Salleo S (2003) Changes in leaf hydraulics and stomatal conductance following drought stress and irrigation in *Ceratonia siliqua* (carob tree). Physiol Plant **117:** 186–194

Maurel C, Boursiac Y, Luu DT, Santoni V, Shahzad Z, Verdoucq L (2015) Aquaporins in plants. Physiol Rev **95:** 1321–1358

McAdam SAM, Brodribb TJ (2014) Separating active and passive influences on stomatal control of transpiration. Plant Physiol **164:** 1578–1586

McKown AD, Cochard H, Sack L (2010) Decoding leaf hydraulics with a spatially explicit model: principles of venation architecture and implications for its evolution. Am Nat **175:** 447–460

Milburn JA (1966) The conduction of sap. I. Water conduction and cavitation in water stressed leaves. Planta **69:** 34–42

Milburn JA, Johnson RPC (1966) The conduction of sap. II. Detection of vibrations produced by sap cavitation in Ricinus xylem. Planta **69:** 43–52

Miyazawa S, Yoshimura S, Shinzaki Y, Maeshima M, Miyake C (2008) Deactivation of aquaporins decreases internal conductance to CO_2 diffusion in tobacco leaves grown under long-term drought. Funct Plant Biol **35:** 553–564

Moshelion M, Halperin O, Wallach R, Oren R, Way DA (2015) Role of aquaporins in determining transpiration and photosynthesis in water-stressed plants: crop water-use efficiency, growth and yield. Plant Cell Environ **38:** 1785–1793

Murray K, Conner MM (2009) Methods to quantify variable importance: implications for the analysis of noisy ecological data. Ecology **90:** 348–355

Nardini A, Ramani M, Gortan E, Salleo S (2008) Vein recovery from embolism occurs under negative pressure in leaves of sunflower (*Helianthus annuus*). Physiol Plant **133:** 755–764

Nardini A, Salleo S (2000) Limitation of stomatal conductance by hydraulic traits: sensing or preventing xylem cavitation? Trees (Berl) **15:** 14–24

Nardini A, Salleo S (2003) Effects of the experimental blockage of the major veins on hydraulics and gas exchange of *Prunus laurocerasus* L. leaves. J Exp Bot **54:** 1213–1219

Nardini A, Salleo S, Raimondo F (2003) Changes in leaf hydraulic conductance correlate with leaf vein embolism in *Cercis siliquastrum* L. Trees (Berl) **17:** 529–534

Nardini A, Tyree MT, Salleo S (2001) Xylem cavitation in the leaf of *Prunus laurocerasus* and its impact on leaf hydraulics. Plant Physiol **125:** 1700–1709

North GB, Martre P, Nobel PS (2004) Aquaporins account for variations in hydraulic conductance for metabolically active root regions of Agave deserti in wet, dry, and rewetted soil. Plant Cell Environ **27:** 219–228

Osborne CP, Sack L (2012) Evolution of C4 plants: a new hypothesis for an interaction of CO_2 and water relations mediated by plant hydraulics. Philos Trans R Soc Lond B Biol Sci **367:** 583–600

Pammenter NW, Vander Willigen C (1998) A mathematical and statistical analysis of the curves illustrating vulnerability of xylem to cavitation. Tree Physiol **18:** 589–593

Pantin F, Monnet F, Jannaud D, Costa JM, Renaud J, Muller B, Simonneau T, Genty B (2013) The dual effect of abscisic acid on stomata. New Phytol **197:** 65–72

Pierce M, Raschke K (1980) Correlation between loss of turgor and accumulation of abscisic acid in detached leaves. Planta **148:** 174–182

Pieruschka R, Huber G, Berry JA (2010) Control of transpiration by radiation. Proc Natl Acad Sci USA **107:** 13372–13377

Pou A, Medrano H, Flexas J, Tyerman SD (2013) A putative role for TIP and PIP aquaporins in dynamics of leaf hydraulic and stomatal conductances in grapevine under water stress and re-watering. Plant Cell Environ **36:** 828–843

Prado K, Maurel C (2013) Regulation of leaf hydraulics: from molecular to whole plant levels. Front Plant Sci **4:** 255

Ribeiro MLRC, Santos MG, Moraes MG (2007) Leaf anatomy of two Anemia Sw. species (Schizaeaceae-Pteridophyte) from a rocky outcrop in Niteroi, Rio de Janeiro, Brazil. Rev Bras Bot Braz J Bot **30:** 695–702

Ritman KT, Milburn JA (1988) Acoustic emissions from plants: ultrasonic and audible compared. J Exp Bot **39:** 1237–1248

Rockwell FE, Holbrook NM, Stroock AD (2014) The competition between liquid and vapor transport in transpiring leaves. Plant Physiol **164:** 1741–1758

Sack L (2010) Leaf pressure-volume curve parameters. PrometheusWiki. http://www.publish.csiro.au/prometheuswiki/tiki-pagehistory.php?page=Leaf pressure-volume curve parameters&preview=10

Sack L, Ball MC, Brodersen C, Donovan L, Givnish TJ, Hacke U, Huxman TE, Jacobsen AL, Jansen S, Johnson DM, et al (2016a) Plant water transport as a central hub from plant to ecosystem function: meeting report for "Emerging Frontiers in Plant Hydraulics" (Washington, DC, May 2015). Plant Cell Environ **39:** 2085–2094

Sack L, Buckley TN, Scoffoni C (2016b) Why are leaves hydraulically vulnerable? J Exp Bot **67:** 4917–4919

Sack L, Holbrook NM (2006) Leaf hydraulics. Annu Rev Plant Biol **57:** 361–381

Sack L, Melcher PJ, Zwieniecki MA, Holbrook NM (2002) The hydraulic conductance of the angiosperm leaf lamina: a comparison of three measurement methods. J Exp Bot **53:** 2177–2184

Sack L, Scoffoni C (2012) Measurement of leaf hydraulic conductance and stomatal conductance and their responses to irradiance and dehydration using the evaporative flux methods (EFM). J Vis Exp **pii:** e4179

Sack L, Scoffoni C (2013) Leaf venation: structure, function, development, evolution, ecology and applications in the past, present and future. New Phytol **198:** 983–1000

Sack L, Streeter CM, Holbrook NM (2004) Hydraulic analysis of water flow through leaves of sugar maple and red oak. Plant Physiol **134:** 1824–1833

Sade N, Shatil-Cohen A, Attia Z, Maurel C, Boursiac Y, Kelly G, Granot D, Yaaran A, Lerner S, Moshelion M (2014) The role of plasma membrane aquaporins in regulating the bundle sheath-mesophyll continuum and leaf hydraulics. Plant Physiol **166:** 1609–1620

Sade N, Shatil-Cohen A, Moshelion M (2015) Bundle-sheath aquaporins play a role in controlling Arabidopsis leaf hydraulic conductivity. Plant Signal Behav **10:** e1017177

Salleo S, Lo Gullo MA, Raimondo F, Nardini A (2001) Vulnerability to cavitation of leaf minor veins: any impact on leaf gas exchange? Plant Cell Environ **24:** 851–859

Salleo S, Nardini A, Pitt F, Lo Gullo MA (2000) Xylem cavitation and hydraulic control of stomatal conductance in laurel (*Laurus nobilis* L.). Plant Cell Environ **23:** 71–79

Sancho-Knapik D, Alvarez-Arenas TG, Peguero-Pina JJ, Fernández V, Gil-Pelegrín E (2011) Relationship between ultrasonic properties and structural changes in the mesophyll during leaf dehydration. J Exp Bot **62:** 3637–3645

Sandford AP, Grace J (1985) The measurement and interpretation of ultrasound from woody stems. J Exp Bot **36:** 298–311

Scoffoni C, Albuquerque C, Brodersen CR, Townes ST, John GP, Cochard H, Buckley TN, McElrone AJ, Sack L (2017) Leaf vein xylem conduit diameter influences susceptibility to embolism and hydraulic decline. New Phytol **213:** 1076–1092

Scoffoni C, McKown AD, Rawls M, Sack L (2012) Dynamics of leaf hydraulic conductance with water status: quantification and analysis of species differences under steady state. J Exp Bot **63:** 643–658

Scoffoni C, Pou A, Aasamaa K, Sack L (2008) The rapid light response of leaf hydraulic conductance: new evidence from two experimental methods. Plant Cell Environ **31:** 1803–1812

Scoffoni C, Rawls M, McKown A, Cochard H, Sack L (2011) Decline of leaf hydraulic conductance with dehydration: relationship to leaf size and venation architecture. Plant Physiol **156:** 832–843

Scoffoni C, Sack L (2015) Are leaves 'freewheelin'? Testing for a wheeler-type effect in leaf xylem hydraulic decline. Plant Cell Environ **38:** 534–543

Scoffoni C, Vuong C, Diep S, Cochard H, Sack L (2014) Leaf shrinkage with dehydration: coordination with hydraulic vulnerability and drought tolerance. Plant Physiol **164:** 1772–1788

Shatil-Cohen A, Attia Z, Moshelion M (2011) Bundle-sheath cell regulation of xylem-mesophyll water transport via aquaporins under drought stress: a target of xylem-borne ABA? Plant J **67:** 72–80

Shatil-Cohen A, Moshelion M (2012) Smart pipes: the bundle sheath role as xylem-mesophyll barrier. Plant Signal Behav **7:** 1088–1091

Sheffield J, Wood EF, Roderick ML (2012) Little change in global drought over the past 60 years. Nature **491:** 435–438

Stiller V, Lafitte HR, Sperry JS (2003) Hydraulic properties of rice and the response of gas exchange to water stress. Plant Physiol **132:** 1698–1706

Taneda H, Kandel DR, Ishida A, Ikeda H (2016) Altitudinal changes in leaf hydraulic conductance across five *Rhododendron* species in eastern Nepal. Tree Physiol **36:** 1272–1282

Taneda H, Terashima I (2012) Co-ordinated development of the leaf midrib xylem with the lamina in *Nicotiana tabacum*. Ann Bot (Lond) **110:** 35–45

Trifilò P, Gascó A, Raimondo F, Nardini A, Salleo S (2003a) Kinetics of recovery of leaf hydraulic conductance and vein functionality from cavitation-induced embolism in sunflower. J Exp Bot **54:** 2323–2330

Trifilo P, Nardini A, Lo Gullo MA, Salleo S (2003b) Vein cavitation and stomatal behaviour of sunflower (*Helianthus annuus*) leaves under water limitation. Physiol Plant **119:** 409–417

Trifiló P, Raimondo F, Savi T, Lo Gullo MA, Nardini A (2016) The contribution of vascular and extra-vascular water pathways to drought-induced decline of leaf hydraulic conductance. J Exp Bot **67:** 5029–5039

Tyree MT, Ewers FW (1991) The hydraulic architecture of trees and other woody-plants. New Phytol **119:** 345–360

Tyree MT, Sperry JS (1989) Vulnerability of xylem to cavitation and embolism. Annu Rev Plant Physiol Plant Mol Biol **40:** 19–38

Tyree MT, Yianoulis P (1980) The site of water evaporation from substomatal cavitites, liquid path resistances and hydroactive stomatal closure. Ann Bot (Lond) **46:** 175–193

Tyree MT, Zimmermann MH (2002) Xylem Structure and the Ascent of Sap. Springer, Berlin

Urli M, Porté AJ, Cochard H, Guengant Y, Burlett R, Delzon S (2013) Xylem embolism threshold for catastrophic hydraulic failure in angiosperm trees. Tree Physiol **33:** 672–683

Vandeleur RK, Sullivan W, Athman A, Jordans C, Gilliham M, Kaiser BN, Tyerman SD (2014) Rapid shoot-to-root signalling regulates root hydraulic conductance via aquaporins. Plant Cell Environ **37:** 520–538

Vicente-Serrano SM, Lopez-Moreno JI, Begueria S, Lorenzo-Lacruz J, Sanchez-Lorenzo A, Garcia-Ruiz JM, Azorin-Molina C, Moran-Tejeda E, Revuelto J, Trigo R, et al (2014) Evidence of increasing drought severity caused by temperature rise in southern Europe. Environ Res Lett **9:** 044001

Wan X, Steudle E, Hartung W (2004) Gating of water channels (aquaporins) in cortical cells of young corn roots by mechanical stimuli (pressure pulses): effects of ABA and of $HgCl_2$. J Exp Bot **55:** 411–422

Woodruff DR, McCulloh KA, Warren JM, Meinzer FC, Lachenbruch B (2007) Impacts of tree height on leaf hydraulic architecture and stomatal control in Douglas-fir. Plant Cell Environ **30:** 559–569

Wu X, Lin J, Lin Q, Wang J, Schreiber L (2005) Casparian strips in needles are more solute permeable than endodermal transport barriers in roots of Pinus bungeana. Plant Cell Physiol **46:** 1799–1808

Wylie RB (1947) Conduction in dicotyledon leaves. Proc Iowa Acad Sci **53:** 195–202

Ye Q, Muhr J, Steudle E (2005) A cohesion/tension model for the gating of aquaporins allows estimation of water channel pore volumes in Chara. Plant Cell Environ **28:** 525–535

Zhang YJ, Rockwell FE, Graham AC, Holbrook MN (2016) Reversible leaf xylem collapse: a potential "circuit breaker" against cavitation. Plant Physiol **172:** 2261–2274